Available online at www.sciencedirect.com
SCIENCE DIRECT®
Vision Research 44 (2004) 2269–2284
Vision Research
www.elsevier.com/locate/visres

Storage for free: a surprising property of a simple gain-control model of motion aftereffects

Wim A. van de Grind [a,b,*], Maarten J. van der Smagt [c], Frans A.J. Verstraten [c]

[a] AG Hirnforschung, Albert-Ludwigs-University, Hansastr. 9, D-79104 Freiburg i.Br., Germany
[b] Functional Neurobiology and Helmholtz Institute, Utrecht University, Padualaan 8, 3584 CH Utrecht, The Netherlands
[c] Psychonomics Department and Helmholtz Institute, Utrecht University, Heidelberglaan 2, 3584 CS Utrecht, The Netherlands

Received 4 August 2003; received in revised form 2 April 2004

Abstract

If a motion aftereffect (MAE) for given adaptation conditions has a duration T s, and the eyes are closed after adaptation during a waiting period $t_w = T$ s before testing, an unexpected MAE of a 'residual' duration T_{rT} s is experienced. This effect is called 'storage' and it is often quantified by a storage factor $\sigma = T_{rT}/T$, which can reach values up to about 0.7–0.8. The phenomenon and its name have invited explanations in terms of inhibition of recovery during darkness. We present a model based on the opposite idea, that an effective test stimulus quickens recovery relative to darkness or other ineffective test stimuli. The model is worked out in mathematical detail and proves to explain 'storage' data from the literature, on the static MAE (sMAE: an MAE experienced for static test stimuli). We also present results of a psychophysical experiment with moving random pixel arrays, quantifying storage phenomena both for the sMAE and the dynamic MAE (dMAE: an MAE experienced for a random dynamic noise test stimulus). Storage factors for the dMAE are lower than for the sMAE. Our model also gives an excellent description of these new data on storage of the dMAE. The term 'storage' might therefore be a misnomer. If an effective test stimulus influences all direction tuned motion sensors indiscriminately and thus speeds up equalization of gains, one gets the storage phenomenon for free.

Keywords: Motion-vision; Motion-aftereffects; Storage; Gain-control model

1. Introduction

If a static test pattern is presented after prolonged adaptation to constant motion of low-to-medium speed, a so-called 'static' motion aftereffect (sMAE) is experienced. This is one of the more extensively studied phenomena of motion vision (reviews: Mather, Verstraten, & Anstis, 1998; Wade, 1994; Wohlgemuth, 1911). Since Exner (1894) and Wohlgemuth (1911), the motion aftereffect (MAE) has most commonly been explained as due to adaptation (gain-control) of motion sensors tuned to the adaptation motion direction (Mather, 1980; Sekuler & Ganz, 1963; Sekuler & Pantle, 1967; Sutherland, 1961). During testing the balance of activity in the total population of motion sensors (together covering all tuning directions) is then shifted towards the opponent direction, causing an opponently directed MAE (Mather, 1980). Here we use a straightforward implementation of this general idea (see also van de Grind, Lankheet, & Tao, 2003; Grunewald, 1996; Grunewald & Lankheet, 1996) and explore the recovery properties of such a model in quantitative detail.

We were initially surprised to find that our model showed 'storage' of the MAE. This phenomenon has traditionally been explained on an intuitive basis by invoking extra 'storage' mechanisms, such as inhibition of recovery in the dark (e.g. Spigel, 1964). We found that the simple implementation of a selective adaptation mechanism described below, implies 'storage', if it is assumed in addition, that test signals stimulate the responsible motion system unselectively. The idea will be explained in detail after an introductory review of the basic psychophysical results. One can characterize the new explanation as follows: Whereas classical

* Corresponding author. Address: AG Hirnforschung, Albert-Ludwigs-University, Hansastr. 9, D-79104 Freiburg i.Br., Germany. Tel.: +49-761-203-9575; fax: +31-49-761-203-9500.
E-mail address: vandegrind@zfn-brain.uni-freiburg.de (W.A. van de Grind).

0042-6989/$ - see front matter © 2004 Elsevier Ltd. All rights reserved.
doi:10.1016/j.visres.2004.04.012

explanations assume that recovery from adaptation is 'normal' during testing and 'delayed' (stored) while the eyes are closed, the present explanation is based on the premise that recovery is 'normal' while the eyes are closed and faster (for the whole system, not for the individual gain controls!) when tested. That this explanation works proves that the term 'storage' for this phenomenon was premature. The mere fact that the overall decay rate *appears* to be slower if testing is delayed, does not necessarily (logically) mean that it is 'stored' during the waiting time. Yet, we will use the term 'storage' (between quotes) to refer to the psychophysical phenomenon, even though our explanation is based on an 'equalization' effect of the test stimulus. Our present analysis should be regarded as a first exploration of an interesting new explanation for the storage-phenomenon, and the first attempt to do this quantitatively with the help of a worked-out mathematical model. The presented empirical tests of the model are suggestive, but further psychophysical work will be necessary. The model's basic structure is compatible with available psychophysical and electrophysiological evidence, as will be explained below. We will first summarize published findings, before turning to the model.

The sMAE has been the only known MAE for more than a century. However, more recently it has been found that there are other MAEs, that can be best perceived if the test stimulus consists of global flicker (Green, Chilcoat, & Stromeyer, 1983) or local flicker, such as dynamic noise (e.g. Blake & Hiris, 1993; Hiris & Blake, 1992), or counterphase-flickering gratings (e.g. Ashida & Osaka, 1995a, 1995b; von Grünau, 1986; Ledgeway, 1994; McCarthy, 1993; Nishida & Sato, 1995). Of these we will discuss the dynamic MAE (dMAE) visible for a test stimulus of non-drifting dynamic noise, after adaptation to moving random textures. Using moving random pixel arrays (RPAs) as adaptation stimuli, we have previously presented evidence that the sMAE and dMAE possibly stem from two relatively independent motion systems, a low-speed system, responsible for the sMAE, and a high-speed system responsible for the dMAE (van de Grind, van Hof, van der Smagt, & Verstraten, 2001; van der Smagt, Verstraten, & van de Grind, 1999; Verstraten, van der Smagt, & van de Grind, 1998; Verstraten, van der Smagt, Fredericksen, & van de Grind, 1999).

An intriguing aspect of the sMAE, but to a lesser extent also of the dMAE, is 'storage'. Suppose an MAE in a given set-up lasts T s. Then, if the eyes are closed during a waiting-period $t_w = T$ s before testing, there still is a 'residual' MAE of $T_{rT} > 0$ s, whereas no such residual MAE was expected. This phenomenon, first described explicitly by Wohlgemuth (1911) and later studied by Griffith and Spitz (1959), was called 'storage' by Spigel (1960, 1962a, 1962b, 1964), who appears to have been unaware of the earlier work. Spigel (1964) inferred from his experiments that the normal rate of aftereffect-decay may be inhibited (so that the aftereffect is 'stored') by the contour-free waiting-period stimuli that he used. He also suggested that stimulus-switching between waiting-period and test period might itself lengthen the residual aftereffect duration. Thus he proposed two explanatory mechanisms: inhibition of aftereffect-decay (also called 'inhibition of recovery'), and transients due to test stimulus switching. It is known from casual observations of the sMAE, that blinking might revitalise an already subsided MAE, a fact that appears to support the idea that transients lengthen MAE-duration.

Inhibition of recovery by the intervening (waiting-period) stimulus now seems unlikely in view of findings reported by Thompson and Wright (1994). They showed that storage occurs even if the intervening stimulus is the same pattern as the test stimulus, only larger. Moreover, they found similar storage for any of 10 different intervening stimulus patterns (storage factors σ of 0.7–0.85). This speaks against inhibition of decay, because such inhibition would have to occur for almost any test stimulus to explain these results. But then it would also work during normal testing. In fact, the one condition that gave somewhat smaller storage, but storage nonetheless (σ values around 0.4), was a situation in which the test pattern itself was used as an intervening stimulus during the waiting-period, albeit demarcated by brief periods of 0.5 s darkness at the start and end of the waiting time. Including the brief dark intervals, the waiting time in this experiment was equal to the normal MAE-duration. These findings appear to exclude inhibition of recovery and to leave only transients due to stimulus-switching as a possible explanation, or more imaginative ideas like MAE storage as a form of association learning (Thompson & Wright, 1994).

Virtually all explanations of MAEs are based on the same general set of ideas. The gain of a direction-selective (and speed-tuned) channel is decreased during adaptation. Consequently all channels that are tuned to the same speed, but to different motion directions, are more sensitive immediately after adaptation than the adapted channel. The amount of adaptation is usually assumed to decrease gradually for tuning-directions differing more and more from the adaptation direction. This leads to a shift of the activity-distribution during testing towards the channels that were least influenced by adaptation, which are channels around the opponent direction (Mather, 1980). This shift in the activity distribution only leads to a percept if all channels are activated simultaneously by a well-chosen test stimulus. Such an assumption is necessary, because darkness does not support the MAE and neither does any other 'wrong' (ineffective) test stimulus. It is the second essential assumption of the present model, the first being that there are automatic gain-control stages in direction-selective

channels. Storage-phenomena already follow from these two assumptions, at least for the gain-control principle used in our model (feed-forward divisive). However, to get quantitative model descriptions of psychophysical results, one needs to implement the two basic requirements in some specific form. An implementation that proves to work well is described below.

Grunewald (1996) and Grunewald and Lankheet (1996) have proposed a network model that includes a quantitative explanation of the finding that an MAE of bi-vectorial transparent motion is uni-directional (van Doorn, Koenderink, & van de Grind, 1984, 1985; Mather, 1980; Verstraten, Fredericksen, & van de Grind, 1994a). Fig. 1A presents a schematic summary of their proposal for one speed and 12 motion directions. Direction-tuned motion sensors of V1, as symbolised by the lower row of circles with arrows that indicate their tuning-direction, project via gain control stages (small circles crossed by oblique lines) to integration units in a higher motion area, such as V5. Weights attached to the projecting excitatory axons (arrows) vary in Gaussian fashion with difference in tuning-direction, keeping the excitatory spread limited to about 45° in direction-tuning difference. Inhibitory influences (black dots) have a much broader Gaussian spread, and are centered on the opponent tuning-direction. Excitatory and inhibitory Gaussian weight distributions are indicated with dotted lines. Only projections from one V1 unit, tuned to the 12-o'clock direction, are shown in Fig. 1, but every motion sensor has a similar projection to the next level's integration units.

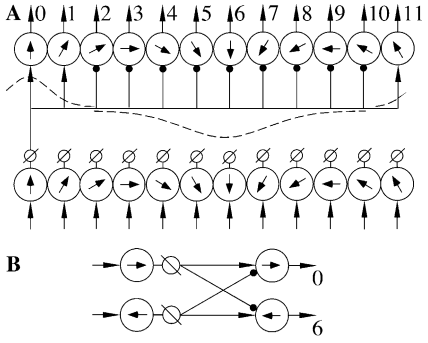

Fig. 1. (A) Basic structure of the Grunewald–Lankheet network model of MAEs. The bottom row symbolises direction-tuned motion sensors in V1, which receive their inputs (incoming arrows) from contrast-sensing neurons. Arrows in the motion sensors symbolise their tuning-direction. Either inherent in the motion sensors or in a subsequent V1 neuron we find the gain-control mechanisms, symbolised with an oblique line crossing a small circle. The motion sensors map via these gain-controls onto integrator units in an extrastriate area, e.g. V5. Sensors with highly similar direction preference converge to excite an integrator neuron, whereas broad inhibition (small black dots) centers around the opponent direction unit of the integrator layer. Excitatory as well as inhibitory connections have weights that change in Gaussian fashion with the difference in direction tuning (interrupted lines). We only show the mapping of the 12 o'clock sensor on the integrator layer, but similar mappings exist for all directions. (B) If we only adapt one direction and therefore only get an opponently directed MAE, as in the experiments described in this paper, we can simplify the network to two-channels. See the text for further details.

If the direction called 0 in Fig. 1 is adapted, its gain will be reduced, so the inhibitory influence on channels around and including opponent direction 6 will decrease. Because these opponent channels do not get an input during adaptation, their lowered inhibition will not be noticeable until the test stimulus is switched on. It is assumed that the test stimulus provides a weak stimulation to all direction-channels. Now, the channels that were pre-adapted (channel 0 and its immediate neighbours) will be less sensitive and thus give a lower output than the disinhibited channels around opponent direction 6-o'clock. This will lead to an MAE in direction 6-o'clock, if we assume that perception follows the most active output channel. For a bi-vectorial transparent motion adaptation, the broad spread of the concomitant two ranges of opponent inhibition ensures a fusion into one aftereffect direction (Grunewald & Lankheet, 1996). If only one adaptation stimulus is used at a time (per trial) and only the opponent MAE needs to be quantified, this network model can be simplified to a two-channel system. Fig. 1B illustrates by way of example, what part of the network is most active and thus directly relevant if we only adapt one direction (e.g. direction 0), and as a consequence get a MAE in the opponent direction (6). Leaving out the influence of neighbouring (non-optimally activated) channels has a quantitative influence that can be compensated by a small increase of the projection weighting factors in the reduced two-channel model. Qualitatively nothing is gained by using the complete multi-channel model to explain results obtained with a single adaptation direction (see also van de Grind et al., 2003). We have carried out simulation studies with these networks in Matlab/Simulink to check the validity of the reduction from 12 (or more) channels to a two-channel model.

A recent electrophysiological study by Kohn and Movshon (2003) in monkey V5 confirms several specific consequences and assumptions of the Grunewald–Lankheet model. For example, like in the model, adaptation in the null direction adapts the gain control of the opponent channel, so it does not change responses to the preferred direction. It only lowers inhibition of the preferred direction by the null direction. Adaptation also lowered the spontaneous firing rate, which can be viewed as a probe of the gain (if spontaneous activation originates before the gain stage). The spontaneous rate (and thus also the gain) recovered exponentially. We left spontaneous firing out of our model, because its influence can be combined with the threshold criterion θ. Nevertheless, it would behave just as reported by Kohn and Movshon, if it were added at the input of the motion sensors or gain control. Spontaneous firing cannot in itself be perceptually suprathreshold, because

otherwise one would see a MAE in the dark, which is not the case. That is the reason why we embed it in the threshold criterion, rather than introducing it explicitly. Kohn and Movshon also find that the gain control must be located in V1, because it has a receptive field size like V1 units, not the larger receptive field size of V5 units. This finding supports the layered structure of the model in Fig. 1, with sensors and gain controls in V1 and the integrator units in V5 (and/or other extrastriate motion areas). Kohn and Movshon also mention that the gain controls in V1 are probably based on processes within the adapted cell, because adaptation in V1 is associated with prolonged hyperpolarisation of non-synaptic origin (Carandini & Ferster, 1997; Sanchez-Vives, Nowak, & McCormick, 2000). Earlier electrophysiological work on MAEs was mostly done on the cat (for a review see Niedeggen & Wist, 1998). The detailed findings on a large variety of cell types are hard to summarise, but the main findings are roughly similar to those discussed above. Various complex cell types in the cat show adaptation properties similar to those of simple cells (Hammond, Mouat, & Smith, 1988). No MAE-phenomena have yet been studied in complex cells of monkeys (which might play a role in the dMAE), and no physiological studies are known to us where dynamic noise is used as a test stimulus after adaptation. It would also be interesting to see MAE-inspired electrophysiological studies in other extrastriate areas than MT.

The ultimate cause of MAEs is the presence of gain-controls, so it is important to develop the gain control stage of our model in sufficient detail. Van de Grind et al. (2003) proposed an explicit circuit to implement this gain control stage, and showed how such a model could quantitatively explain the relation between nulling-thresholds and MAE-durations for the dMAE. Fig. 2 presents this divisive feedforward gain-control model. In the present paper we will show that this model can also explain storage phenomena. Interestingly, even though gain-controls based on multiplicative or subtractive principles can be used to explain the occurrence of MAEs (van de Grind et al., 2003), they do not give 'storage' phenomena for free, as the divisive gain control of Fig. 2 does.

It should be kept in mind that the two illustrated 'channels' in Fig. 2 are part of a larger population and that the detection criterion of Fig. 2 is a two-channel limit of a population criterion, comparing many channels of different direction and speed tuning. In Section 2 we first provide an outline of the model, then a mathematical description. In Section 3 the model is tested using storage-data for the sMAE published by Spigel. These are averaged results of 50 subjects, and Spigel used rotation rather than linear motion. Therefore we did a psychophysical experiment (Section 4) to measure residual sMAE duration for individual subjects and translatory motion as a function of waiting time t_w.

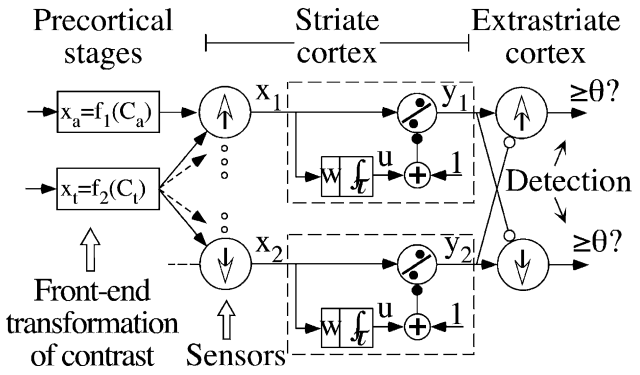

Fig. 2. Two opponently direction-tuned channels are shown (enclosed by interrupted lines) out of a population representing all directions. At the output, a detector detects and flags the channel that reaches an activity value θ units above the population mean. At the input, we have symbolised the storage experimental paradigm. This starts with selective adaptation, of one channel only, during t_A s. After adaptation there is a waiting time of t_w s, before the test stimulus is switched on, and stimulates all (here both) channels. Each channel consists of an automatic gain-control with a gain $1/(1+u)$, where u is the output of a feedforward leaky integrator loop.

Because model parameters have been estimated previously for the dMAE (van de Grind et al., 2003) it is also possible to test storage predictions for the dMAE. Section 4 therefore also presents results on the dMAE, and then shows that our model works equally well for dMAEs and sMAEs, but requires different parameter values for the responsible networks. Notably, the time constants of gain controls in low-speed channels, which we hold responsible for the sMAE, must be substantially longer than those in high-speed channels, responsible for dMAEs. Moreover, unlike the latter, the former system responds to static test patterns. Conversely, only high-speed units are sensitive to dynamic noise test stimuli. (See also Fig. 1 in van de Grind et al., 2001, which shows that static spatial noise patterns only rival binocularly with low speeds, whereas dynamic noise patterns only rival with high speed motion.)

2. A gain-control model of MAEs and of MAE-storage

2.1. Outline of the model

Fig. 2 presents the basic structure of our model, in which gain-control stages of a pair of opponently direction-tuned motion channels are the main players. The gain of each channel can be lowered relative to its resting value of 1 by charging a leaky integrator (RC-integrator) with time constant τ. Channel-gains g are defined as $1/(1+u)$ where u is the output signal of the channel's leaky integrator. Suppose that the upper gain-control in Fig. 2 is adapted by some constant input signal, so that its gain is reduced. At the end of adaptation the adapted channel's gain g_1 will recover

exponentially with time constant τ. During testing both (all) channels are stimulated equally, but the upper channel is still less sensitive, so the lower channel, with initial gain $g_2 = 1$ will give the stronger output. In a detector it is decided whether or not the difference in output between the two channels (y_2–y_1 as indicated in Fig. 2) exceeds a threshold criterion θ. If it does, motion is seen in the winner's direction, if not no motion is seen. This is all there is to the model, yet we will demonstrate that it produces storage phenomena like those reported in psychophysical studies.

What are the input sources of our gain-control model? In the front-end visual system motion is first detected by motion sensors, such as simple cells—sensitive to extended contours, edges or gratings—or complex cells, some of which might mainly signal texture motion. Resulting motion signals of appropriate direction-specificity enter the upper input of our gain-control model, and thereby decrease gain g_1 (Fig. 2). We will call this adaptation input signal x_a and the duration of adaptation t_a. Input signals to the model, symbolised by the letter x, are always limited to the range 0–10 units. Although the gain-control principle is in itself multipurpose, we assume in the present context that x is a function of motion parameters and contrast. The somewhat arbitrary choice of the signal-range (0–10) does not influence results, since the mapping of visual stimuli onto model signals has to include a constant (speed-specific) gain factor that can be chosen appropriately (van de Grind et al., 2003). The test signal x_t is of a different kind for the two types of MAE: a static pattern for the sMAE and dynamic noise for the dMAE. In both cases we assume that the test stimulus excites all direction-tuned channels of the model, here both channels, about equally. This is reasonable since the test stimuli 'contain' all motion-directions with equal energy, which is the reason why they are not seen to move if presented without pre-adaptation. Networks tuned to other speeds are identical, except for their parameter values. We assume that the same model structure holds both for the dMAE and for the sMAE, but with different parameter values and with a different selectivity for non-motion inputs (dynamic versus static tests).

The gain-controls of Fig. 2 have only two parameters, namely weighting factor (fixed gain) w at the leaky integrators' input, and time constant τ. The detection stage adds another parameter θ, the detection threshold. In the following formal model-exposition we emphasize the role of two of these model parameters (w and θ), and the input signal characteristics, notably test signal strength x_t. All durations will be expressed in τ-units, so that τ is just a temporal scaling parameter (see below). Parameter w determines the minimum gain-factor after prolonged maximal adaptation, which equals $1/(1 + wx_a)$. According to van de Grind et al. (2003) w probably has some value around 0.5 and τ is on the order of 2–3 s for the dMAE. The time constant for low speed channels, responsible for the sMAE, is probably substantially larger, e.g. 10–30 s (see later). We have proposed such a feedforward divisive gain-control a long time ago (e.g. van de Grind, Grüsser, & Lunkenheimer, 1973; van de Grind, Koenderink, & Bouman, 1970; van de Grind, Koenderink, van der Heyde, Landman, & Bouman, 1971) to account for Weber's law of dark adaptation, and highly similar gain-control principles for contrast are nowadays often called 'normalisation'. Carandini, Heeger, and Movshon (1997) pointed out that shunting inhibition is divisive and tested the divisive gain-control principle with extracellular recordings in V1 of macaques. Similarly van de Grind, Lankheet, van Wezel, Rowe, and Hulleman (1996) applied the idea to describe (luminance-dependent) gain-control in horizontal cells of the cat retina. A feedforward divisive gain-control is therefore not beyond the capabilities of local neural circuits, and often describes their behavior very well.

2.2. Mathematical description of the model

At any given time t the gain of each channel equals $1/(1 + u(t))$, where $u(t)$ is the output signal of the channel's leaky integrator at time t. Output $y(t)$ is the product of input $x(t)$ and gain $(1 + u(t))^{-1}$, so: $y = x/(1 + u)$, where y, x, and u are functions of time t. During an adaptation period of t_a s duration, the upper channel's leaky integrator in Fig. 2 will charge and reach a final value

$$u_a = wx_a\{1 - \exp(-t_a/\tau)\} \tag{1}$$

where u_a is the value of $u(t)$ at $t = t_a$, that is, at the end of adaptation. This is simply the response of an RC-circuit to a step function. The derivation of this formula is treated in almost every textbook on electrical engineering, as is that of the formula used below for the response to an off-step (the leak-relation used in formula (2)). RC-circuit behavior is ubiquitous in the nervous system, the best known example being the neural membrane.

If we do not immediately test after adaptation but insert a stimulus-free waiting period of duration t_w then the output of the adapted leaky integrator at the start of testing will be

$$\begin{aligned} u^* &= u_a \exp(-t_w/\tau) \\ &= wx_a\{1 - \exp(-t_a/\tau)\} \exp(-t_w/\tau) \end{aligned} \tag{2}$$

When a test stimulus x_t is switched on, the leaky integrators of all channels will start to charge according to $w \cdot x_t\{1 - \exp(t/\tau)\}$ where t is now time since the start of testing. (For reasons of notational simplicity we will not write $x_t(t)$, because it is assumed that x_t is constant during the test interval, that is from time $t = 0$ onward.)

From the start of testing, that is for $t \geqslant 0$ we have the following gains of the two channels as a function of testing time t:

$$g_1 = 1/(1+u_1) \quad \text{with}$$
$$u_1 = wx_t(1-\exp[-t/\tau]) + u^*\exp[-t/\tau] \tag{3a}$$

$$g_2 = 1/(1+u_2) \quad \text{with } u_2 = wx_t(1-\exp[-t/\tau]) \tag{3b}$$

In writing down these formulae we used the superposition principle, because leaky integrators are linear systems (which the gain control as a whole is not). Therefore leak and charge terms can be added. At time $t = T_r$, when the residual MAE (of duration T_r) ends, the difference between $y_2 = g_2x_t$ (output of the lower channel in Fig. 2) and $y_1 = g_1x_t$ (output of the upper channel) will just equal θ, so we have

$$g_2 - g_1 = \theta/x_t \quad (\text{at } t = T_r) \tag{4}$$

If we insert (3a) and (3b) in (4) and solve for T_r/τ (see Appendix A), we get

$$T_r/\tau = \mathrm{Ln}\{(B+\sqrt{D})/(2A)\} \tag{5a}$$

with

$$A = (1+wx_t)^2 \tag{5b}$$

$$B = (1+wx_t)(2wx_t - u^*) + u^*x_t/\theta \tag{5c}$$

$$C = wx_t(wx_t - u^*) \tag{5d}$$

$$D = B^2 - 4AC \tag{5e}$$

and u^* as defined in formula (2).

The first thing to note about formulae (5a–e) and (2) is that time constant τ merely acts as a temporal scaling parameter. It is therefore most convenient to express all temporal values in τ-units. For example, an MAE-duration of 0.5 then means $T = 0.5\tau$. The ratio of residual MAE-duration measured for $t_w = T$ (that is $T_r(T)$ or abbreviated T_{rT}) to the normal MAE-duration T (for $t_w = 0$) will be called the 'storage factor' $\sigma = T_{rT}/T$. This storage factor will not be influenced by the choice of τ (normalising both T_{rT} and T with τ gives the same ratio σ). This means that storage strength only depends on two model parameters, w and θ, and of course also on the stimulus parameters x_t, x_a. Stimulus parameter t_a does not usually play a role, because adaptation duration is mostly kept constant in psychophysical experiments. It is often even 'long enough', say three or more time constants, to make the factor $\exp(-t_a/\tau)$ in (1) and (2) negligeably small.

To visualize the processes that lead to storage in this model we plotted the gains g_1 and g_2 as a function of normalised time t/τ in Fig. 3. Model parameters were chosen to give a significant storage factor σ of around 0.6. These otherwise quite arbitrary parameters were $w = 0.6$, $\theta = 0.7$, $x_t = 1.4$, $x_a = 10$. For these choices the normal MAE-duration ($t_w = 0$) is about 0.6τ, as

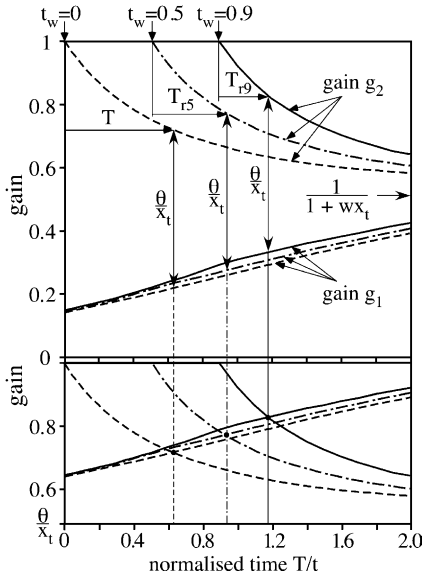

Fig. 3. Possible time courses of gain recovery after adaptation, that is during the waiting time and testing periods. In the upper panel three possible testing regimes are symbolised, testing directly after adaptation ($t_w = 0$), after a waiting time of 0.5τ and of 0.9τ, where τ is the time constant of the leaky integrators of Fig. 2. As soon as the corresponding gain curves for the upper and lower channel of Fig. 2 (g_1 respectively g_2) approach each other to within a distance of θ/x_t the residual MAE ends (see formula (4) of the text). This leads to the respective residual durations T, T_{r5} and T_{r9} for the three illustrated stimulus regimes of testing at $t_w = 0$, $t_w = 0.5\tau$ and $t_w = 0.9\tau$. In the bottom panel the g_1-curves are shifted upwards by an amount of θ/x_t so that the criterion of formula (4) translates into gain-curve crossings.

calculated with (5a)–(5e). Fig. 3 presents gain-time functions for three different choices of the waiting time: $t_w = 0$, $t_w = 0.5\tau$, and $t_w = 0.9\tau$. In Fig. 3 the residual MAE-duration after a waiting time of 0.5τ is denoted as T_{r5} and that after a waiting-period of 0.9τ as T_{r9}. Formula (4) gives a criterion, illustrated by vertical double arrows in Fig. 3 (upper panel): residual MAEs end as soon as the distance between two corresponding g_1 and g_2 gain functions equals θ/x_t. Therefore, if we shift the lower gain functions (g_1) upward by an amount θ/x_t, as in the lower panel of Fig. 3, the residual MAEs end where the shifted gain-curves g_1 cross the corresponding g_2-curves. It is clear from Fig. 3 that adaptation of the unadapted channel to the test stimulus (g_2) has a major influence. The later we start to test, the more the g_2-curves are shifted to the right in Fig. 3, and thus the later in time after adaptation the MAE ends. Both gains eventually converge on the value $1/(1+wx_t)$. This follows from formulae (3a) and (3b) for increasing t, when $\exp(-t/\tau)$ goes to zero. Because both gain values converge on the same limiting value their difference goes to zero, so it seems reasonable to call this an 'equalization' effect of testing. A consequence of the model is that the test stimulus lowers the gain for all directions. There is indeed psychophysical evidence for this phenomenon and we will come back to it in Section 6.

Fig. 3 shows that gain g_1 courses exponentially towards its unadapted value of 1 during the stimulation-free waiting period, but then shifts its final goal to the lower value $1/(1+wx_t)$ as soon as we start to test. However, the previously unadapted opponent channel will also adapt to the test stimulus and its gain will also converge on $1/(1+wx_t)$. This means a shortening of the time until g_1 approaches the gain values of the other channels (here g_2) to within a criterion distance, and thus of the measurable aftereffect of adaptation. In conclusion: the psychophysical 'storage' effect can be explained with a model in which its cause has nothing whatsoever to do with slowing down of recovery during the waiting interval. On the contrary, passive exponential recovery of the adapted channel with its normal time constant towards its resting value, occurs *only* during darkness or when looking at a neutral stimulus that does not excite the motion channels. Equalization of gains is caused by a test stimulus that excites all motion channels unselectively, even if this excitation is weak. The residual MAE ends when the output signals of all direction-tuned channels of a considered speed become mutually equal to within a criterion difference θ. This equalization will occur later in time (reckoned from the end of adaptation), if we start to test after a longer waiting-interval, provided this does not exceed some limit. (To be more exact: provided gain g_1 has not yet reached the value $1-\theta/x_t$ when we start testing, as can be inferred from Fig. 3.)

This illustrates how a simple mechanism that has (often implicitly) been presumed to be the cause of MAEs, explains 'storage' without any inhibition of decay, transients or conditioning effects. Of course it might very well be that such additional effects also play a role, but parsimony dictates that we first explore the explanatory scope of the equalization effect. Let us therefore do a parametric study of the model's behavior, using the above-mentioned 'storage-factor' σ as a summary of 'storage' strength. This factor has often been used in psychophysical studies (e.g. Thompson & Wright, 1994), albeit under various other names. Storage factor σ and normalized MAE-duration T/τ prove to be inversely related in our model, which means that a maximum value of σ is obtained for any given combination of the parameters θ and w for which T/τ goes to zero.

We calculated σ and θ as a function of w for a series of fixed values of T/τ (including 0), using a Mathematica notebook containing among others formula (5a)–(5e). This led to the graphs in Fig. 4, where the upper panels give σ as a function of w for constant normalised MAE-durations ($T/\tau \in \{0, 0.25, 0.5, 0.75, 1, 1.25, 1.5\}$), whereas the lower panels present θ as a function of w, for the same cases as the upper panels. Adaptation strength x_a is set at its maximum value of 10. In the left hand panels the test strength $x_t = 0.5$, in the right hand panels $x_t = 1$. Remember that we think of this test strength as the stimulation of slow motion channels by a static pattern (the sMAE) or of fast channels by dynamic noise (dMAE). Therefore we expect test stimulation strength x_t to be substantially smaller than the maximum stimulation by motion of the proper direction and speed (which has a value of 10 in the model). A value like $x_t = 1$ means 10% of the maximum stimulation by an optimal motion stimulus and is therefore already quite strong for a 'non-adequate' stimulus. In the lower panels we plotted θ/x_t on the ordinate rather than θ to be able to use the same scale for both lower graphs.

Fig. 4 immediately shows that for a given value of w, the fixed input gain of the leaky integrator stage, storage factor σ always increases for decreasing MAE-durations (increasing θ). If two observers with the same parameters of their gain-controls (w and τ) have different detection criteria, that is different values of θ, the subject with a shorter MAE-duration (higher θ) would have the stronger storage: Fig. 4. It was shown by van de Grind et al. (2003) that the ratio between MAE-strength (nulling threshold) and direction discrimination threshold depends directly upon w, so that w can in principle be determined in psychophysical experiments. These authors also showed how τ can be measured and for the dMAE their results suggest that $w \approx 0.5$ and $\tau \approx 3$ s. Because the dMAE-duration is usually 2–3 times this time constant, we have a value for T/τ of at least 2, which according to Fig. 4 should lead to rather small storage values (σ around 0.2–0.3). For the sMAE, Verstraten, Fredericksen, Grüsser, and van de Grind (1994b), using moving random pixel arrays as adaptation, mention values for τ of 32 and 40 s. If this is about right, most reported sMAE-durations are on the order of 0.5τ, which in Fig. 3 corresponds to the curves marked with closed circles. These curves show that σ-values of 0.6–0.85, as reported in the storage literature (for the sMAE) can be obtained at higher w and x_t-values. Given such choices of parameter values, the model can explain storage for both the sMAE (high storage factors) and the dMAE (low storage factors). Moreover, these are not free model-fitting exercises, because high values for w and x_t, as for the sMAE, have implications for the relation between MAE-strength and motion detection (or direction discrimination) thresholds (van de Grind et al., 2003). Any choice of parameter values has consequences beyond the storage factor per se, and can therefore be tested in appropriately designed experiments. Admittedly, these additional experiments have not yet been done. It would be imperative to do a wide range of tests on the same subjects and forego averaging across subjects to really test the present model adequately. This must be left to the future. Here we perform one test of the model, its ability to describe storage data. In a previous paper

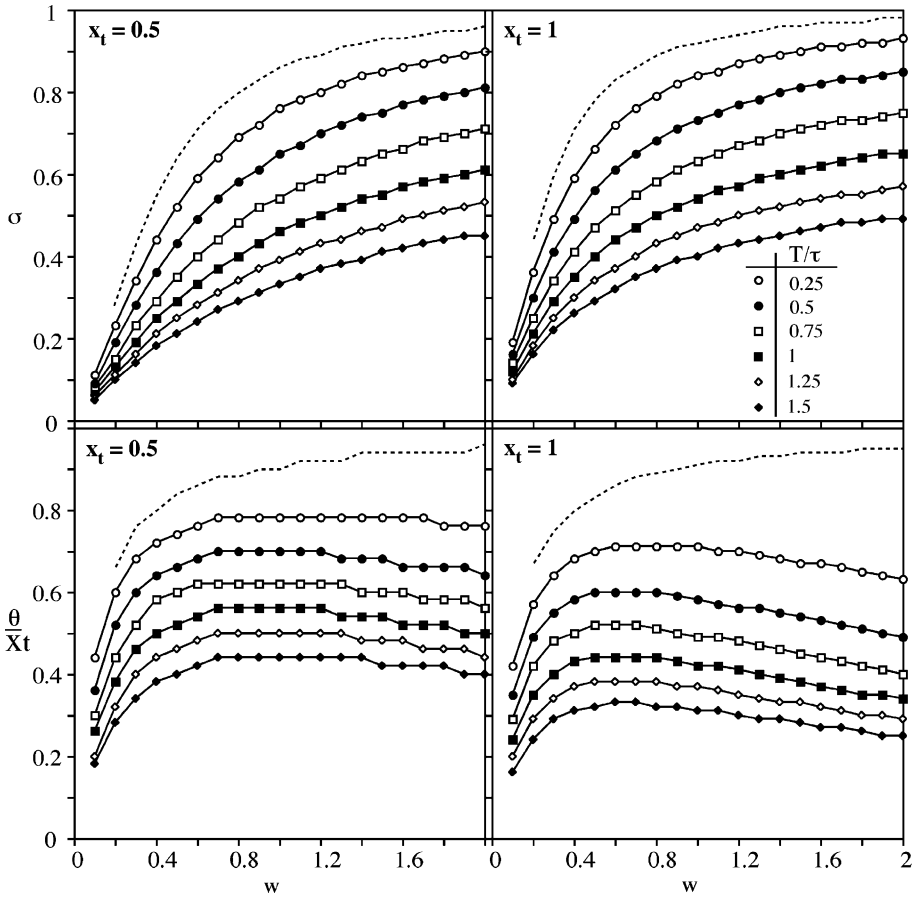

Fig. 4. Storage factor σ (upper panels) and the criterion ratio θ/x_t calculated as a function of w for a range of values of T/τ, as given in the inset table in the upper right hand panel. The left hand column represents the case of test stimulus strength $x_t = 0.5$, the right hand column for $x_t = 1$. Given a storage factor σ, one can draw a horizontal line to find the crossing point with one of the T/τ-curves, read off the corresponding w value in the upper panels, and then at that w-value the corresponding θ/x_t value in the lower panels. In this way one can estimate parameter values leading to a given storage factor and also see what is possible and what not.

boundary conditions were set on the parameters for describing the dMAE and these will be respected below.

3. Testing the sMAE-model with published 'storage'-data

Spigel (1962b) presented an interesting quantification of the storage-effect that goes a step beyond the mere use of storage factor σ. He plotted residual MAE-duration T_r as a function of the duration t_w of a stimulus-free waiting-interval (darkness in his case). Such a curve $T_r = f(t_w)$, which we will call a 'Spigel-function', provides more information on the (normally hidden) gain-restoration process than a single number such as σ. We can of course calculate these curves for our model and they can be conveniently measured in a psychophysical experiment. To illustrate these Spigel-functions and their use we will first fit Spigel's own findings with our model. Spigel (1962b) used a "rotating disc containing a black-and-white radial pattern" as adaptation stimulus and measured residual sMAE-duration T_r of the ensuing rotational sMAE (after waiting-interval t_w). Spigel then fit his results with the relation $T_r = T - kt_w/T$, and found that $T = 8.94$, $k = 2.22$ gave an optimal fit. Unfortunately he did not give the results separately for each of his 50 subjects, so we have to use the published grand average across subjects. His linear fit shows that T_{rT} equals $8.94 - 2.22 = 6.72$ for $t_w = T = 8.94$ s, so that $\sigma = 6.72/8.94 = 0.75$. From Fig. 4 we see that—as an example—the curve for a normalised MAE-duration $T/\tau = 0.5$ could give $\sigma = 0.75$ for $w \approx 1.6$, $\theta \approx 0.33$ and $x_t = 0.5$ or at $x_t = 1$ for $w \approx 1.2$ and $\theta \approx 0.56$. In Fig. 5 we plot the curves $T_r = f(t_w)$ for these two parameter sets and $T = 8.94$ s, $\tau = 17.88$ s (so that $T/\tau = 0.5$). Spigel's data points (from Fig. 1 in Spigel, 1962b) are included in the figure.

We measured Spigel's data with a caliper from an enlarged version of his Fig. 1, but found an inconsistency in the drawing. If the line in his Fig. 1, which is supposed to represent regression line $T_r = 8.94 - 2.22t_w/T$, is extended to the ordinate it gives an intersection $T = 8.1$ s rather than $T = 8.94$. To resolve this

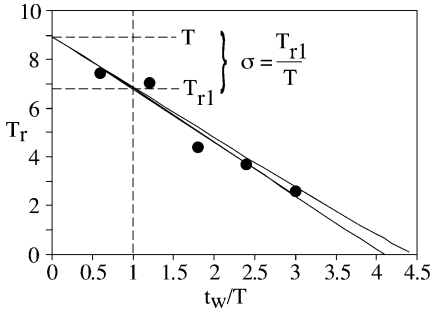

Fig. 5. Two examples of calculated Spigel-curves (defined in the text) for the sMAE, compared to the data points of Spigel (1962b). From Spigel's regression line description we calculated the storage factor σ and then found the model parameters giving such a storage value from the graphs in Fig. 4, as described in the legend to Fig. 4. With these parameters we calculated Spigel functions for our model with the formulae given in the text. They fit the data points quite well, illustrating the descriptive power of our model.

discrepancy, we have assumed that his formula was correct and that the ordinate's scale was drawn inaccurately. This meant that we had to shift his data points and his graphical linear fit slightly upwards. After this correction the data points could be translated into numbers. The results are included in Fig. 5 as black circles and the best fit through these points is $T_r = 8.95 - 2.18t_w/T$, which is close enough to Spigel's summary of his data. The straight lines in Fig. 5 represent the functions $T_r = f(t_w)$ as calculated from our model equations for the parameter values given above at $x_t = 0.5$, respectively $x_t = 1$. It is clear that our model can easily capture the pattern of results reported by Spigel (1962b).

Fig. 5 also shows that the model-functions $T_r = f(t_w)$ are—at least for the chosen parameter values—almost perfectly linear. Linear fits correlated with $r^2 = 0.9998$ to the model functions. This makes 'Spigel'-functions $T_r = f(t_w)$ attractive in psychophysical experiments on 'storage'. Yet, Spigel functions for our model are only linear in the parameter range relevant to describe Spigel's psychophysical data. For example, if we decrease θ, keeping the other parameters as mentioned above, the model's Spigel curves get more and more curved in such a way, that they decrease faster in the beginning (low t_w-values) and slower towards the end (high t_w-values). As indicated in Fig. 5 the value of storage factor σ can also be determined from Spigel-functions, but it represents only a single point on the function, and as such is less informative than complete Spigel-functions. Still, the value of σ for Spigel's data, 0.75, corresponds closely to values reported for sMAE-storage by others. Of course, to the extent that Spigel-functions are linear, storage factor σ together with the directly measured MAE-duration T, in principle give the same information as a Spigel function. However, measuring the complete function makes it possible to check how well a linear regression fits the function and gives a more reliable estimate of the slope and thus σ. As mentioned above Thompson and Wright (1994) reported σ-values between 0.7 and 0.85 for 10 different types of waiting-time stimuli. Both these data and the findings of Spigel can be described by our model, but require higher values of w, θ and τ than those reported for modelling the dMAE (van de Grind et al., 2003). Therefore the questions arise, whether the model can also describe storage phenomena for the dMAE, and what Spigel functions for the dMAE look like. We have found no Spigel functions for the dMAE in the literature, so we decided to measure them in the following psychophysical experiment. Similarly, we wanted to provide some Spigel-functions for the sMAE and translatory motion for individual observers, because we have not found such data in the literature either.

4. Psychophysical quantification of storage for sMAE and dMAE, as measured with translatory random texture motion

4.1. Methods

4.1.1. Apparatus and stimuli

Moving random pixel arrays (RPA) were generated by a custom-built moving-noise-pattern generator, controlled by a Macintosh computer. Patterns were presented on a CRT display (ElectroHome model EVM-1200, P4 phosphor) at a display rate of 90 Hz. The waiting-period stimulus was darkness and for a dMAE the ensuing test stimulus was dynamic visual noise with a cut-off temporal frequency of 45 Hz. This means that all the pixels of an RPA are simultaneously randomly refreshed every 22 ms to obtain dynamic noise. For the sMAE we used a static RPA as test stimulus. Average luminance of the screen was 50 cd/m^2 during stimulus presentation and 0.1 cd/m^2 during 'darkness'. Root-mean-square contrast of the RPAs was 0.7 (70%).

4.1.2. Procedure

Observers were presented with a pattern moving horizontally to the left or to the right for $t_a = 30$ s with one of two speeds in the range of speeds where the dMAE is strong, viz. 11.28, or 19.74 deg/s, and one speed of 1.41 deg/s to measure MAE-durations for the sMAE. After 30 s adaptation to one of these speeds, the screen was dark for t_w s, after which the residual MAE-duration was measured with a dynamic noise stimulus for the dMAE and with a static noise pattern for the sMAE. For $t_w = 0$ s the residual MAE equals the normal MAE, of course. Observers were warned by one beep at the start of the waiting period and one beep when they had to start timing the residual MAE. For $t_w = 0$ the subjects thus heard two beeps at a time. After

a subject indicated the end of a residual MAE with a button-press or the absence of a MAE (by pressing another button), a 30 s pause was given. The conditions were presented in a pseudo-random sequence. Viewing distance was 1 m, resulting in a square display with sides of 8° of arc. Viewing was binocular and a fixation point was present in the center of the display. Head support and a chin rest were provided. All conditions were presented at least six times in a darkened room.

4.1.3. Observers

Two experienced and informed observers, the authors MS and WG, and a naive observer (IV) participated in the dMAE measurement. The naive observer was given some training on a random selection of the experimental conditions to allow her to become familiar with the set-up and procedures. The sMAE-data were obtained one year earlier during an experiment in which all three authors were the experienced and informed observers. An experienced additional observer (PH) participated without being informed about the purpose of the experiment.

5. Results

5.1. Storage of the sMAE for linear random texture motion

We measured at least six T_r-values for each of seven waiting-time values between 0 and 15 s and determined averages and standard errors of the mean for the T_r-values at each of these seven t_w values. To minimize the influence of noise still further we applied a three-point smoothing algorithm to the seven-point Spigel functions for each of the four subjects. The results are presented in Fig. 6. In order to get a clearer presentation we shifted the Spigel-curve of subject PH in Fig. 6 a factor of two downward. Without this shift the rather flat curve of PH mingles with the last three points of the steeper curves for WG and MS, after the shift it is clearer that PH and FV have similarly flat curves, that is more 'storage', than WG and MS. The regression lines fitting the data in Fig. 6 and the corresponding storage factors are as follows:

$$\begin{aligned}
&\text{MS:} && T_r = 16.07 - 0.71t_w && (r^2 = 0.986) \rightarrow \sigma = 0.29\\
&\text{WG:} && T_r = 16.03 - 0.70t_w && (r^2 = 0.891) \rightarrow \sigma = 0.30\\
&\text{FV:} && T_r = 6.32 - 0.26t_w && (r^2 = 0.918) \rightarrow \sigma = 0.74\\
&\text{PH:} && T_r = 10.63 - 0.25t_w && (r^2 = 0.978) \rightarrow \sigma = 0.75
\end{aligned}$$

The linear fits are good to excellent. The storage factors σ can be read from the regression formulae, because $T_r = T - m \cdot t_w$ means that $\sigma = 1 - m$. From this we find storage factor values of 0.29, 0.3, 0.74, and 0.75, for MS, WG, FV, and PH, respectively. This is a remarkable result, because it shows clearly that the amount of storage is strongly subject-dependent and that averaging across subjects would mask these large individual differences.

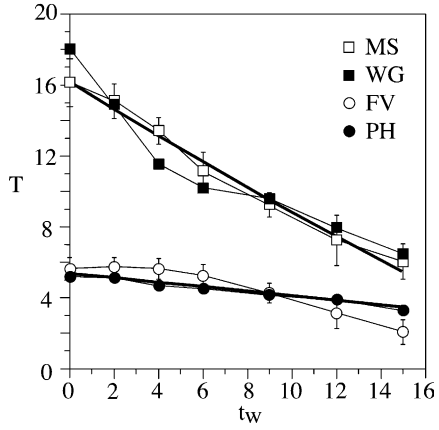

Fig. 6. Spigel functions for the sMAE and four subjects. Adaptation speed was 1.41 deg/s. Two subjects (open and closed circles) had relatively strong 'storage' (σ-values of 0.74 and 0.75), the other two showed less storage (0.29 and 0.30). Standard errors of the mean are given for two subjects (open squares and open circles), but were similar for the other two subjects. The T_r-values for PH were all halved (scaled down), to bring her curve close to that of subject FV. This enables a direct comparison of the data for FV and PH, the two subjects with a large storage factor. Linear regression lines, as defined in the text, describe the results quite well, even though some data-curves appear to be slightly convex and others concave. Thick black lines are Spigel functions for the model, with parameters to fit the results of PH (her Spigel function is also scaled down, of course), and MS.

To describe the psychophysical results with our model we proceeded as follows. We started from the parameter values obtained by fitting Spigel's data in the previous section (Fig. 5): $\tau = 18$ s (Spigel's value rounded), $x_a = 10$, $t_a = 2\tau$ (most experiments use about half a minute of adaptation time), $x_t = 1$, and the important parameters $w = 1.2$ and $\theta = 0.56$. Our aim was to fit the results of all subjects by just varying w and θ, that is by moving through the data space shown in Fig. 4. This proved to be rather easy, because one can fine-tune σ by changing w, which means moving along the upper right hand curves of Fig. 4 (for which $x_t = 1$). If this does not change σ sufficiently or if the T-values (ordinate-intercepts of Spigel-functions) are too low or high one can change the ratio T/τ by changing θ, which means moving vertically from curve to curve in Fig. 4. In this way we could fit the data of Fig. 6 by eye with the following parameter choices: MS: $w = 0.289$, $\theta = 0.397$; WG: $w = 0.297$, $\theta = 0.403$; FV: $w = 0.85$, $\theta = 0.640$; PH: $w = 1.45$, $\theta = 0.490$. The model curves for MS and PH are included in Fig. 6 to illustrate the quality of this description. The model curve for MS, who has a lower storage factor than PH, deviates slightly from linearity in the same direction as his data (and those for WG).

In the range where Spigel functions are linear, we only need two parameters to fit them to a data set, one to manipulate the slope and one to choose the vertical position (the value of T). The parameters w and θ both

influence slope as well as T/τ values. To get a better understanding of the parameter interactions, we calculated curves of constant storage value σ in w–θ-space, as shown in Fig. 7 (falling curves with thin or interrupted lines). Along these loci of constant σ, the values of T/τ change. As long as we do not know T/τ, we cannot therefore uniquely determine the best values of w and θ for a given subject. This shows that an independent experiment is necessary to fix T/τ and get a unique fit of the model to the data. To illustrate that the fit would be unique if T/τ were known, we also included some curves of constant T/τ in Fig. 7 (rising curves, thick lines). Where the curve of constant σ that describes the data best crosses the curve for the best fitting T/τ-value, we find the unique best values of w and θ. Let us now look at the model fits for FV and PH given above, and compare them with the fit to Spigel's own data, described in the previous section. All three fits are represented by points in w–θ-space in Fig. 7. It is immediately clear from this representation, that Spigel's data and those for FV and PH all roughly fall along the same constant-σ curve (σ about 0.75), but that they are in different ranges of T/τ-values. This means we could have decided to fit the data for FV and PH with the same w and θ values as found for Spigel's data by using different τ-values in the three cases.

It is obvious even without the model, that one cannot deduce τ-values from a 'storage'-experiment alone, which therefore does not completely characterise the MAE-properties of subjects. Any model of MAE-storage would make this problem explicit. Therefore we do not see it as a shortcoming of our model that the storage-data in themselves do not allow a unique fit. The model, as it is, gives the best available description. It is the first quantitative model of the 'storage' phenomenon, and it shows that assumptions like 'inhibition of decay' in the dark are not necessary. No extra 'storage' mechanisms are necessary, we only used leaky integrators with one single time constant that did not change at any time. To uniquely fit the model to data of individual subjects one needs additional (independent) psychophysical data to estimate time constant τ. Using a reasonable average value of τ from the literature, we were able to fit all available storage data quite well.

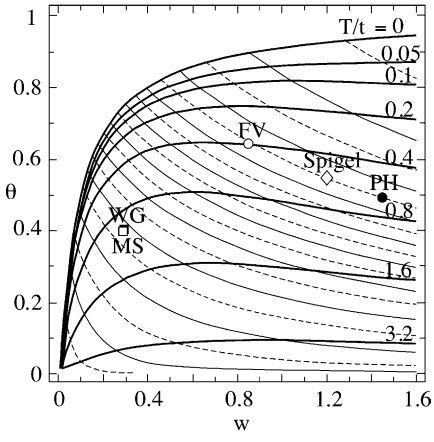

Fig. 7. For constant values of adaptation and test stimulus strength ($x_a = 10$, $x_t = 1$), and constant adaptation duration t_a ($= 6\tau$) we calculated lines of constant storage value σ in θ–w-space. These are the falling curves, starting at the bottom left for $\sigma = 0.05$, then $\sigma = 0.1$, 0.15, 0.2, etc. until the top right curve for $\sigma = 0.95$. These curves are alternately drawn as continuous and interrupted lines to make it easier to visually find the line for a specific σ-value. Rising thick black curves are lines in θ–w-space of constant T/τ-value. We chose the values 0 (no MAE), 0.05, 0.1, 0.2, 0.4, 0.8, 1.6, 3.2, as indicated at the top right of each curve. The w–θ values that provided the best fits to the data in Fig. 6 for FV (open circle), PH (filled circle), MS (open square) and WG (filled square) are included.

5.2. Storage of the dMAE for linear random texture motion

The main results of our experiments on the dMAE are given in Fig. 8, where the panels A–C show data for observers WG, IV, and MS, respectively. Despite the fact that two of the subjects have many years of experience with this type of experiment (measuring MAE-durations), the standard deviations are substantial. Every data point is the average of 10 measurements for WG, eight measurements for IV and six measurements for MS. Subject IV had very brief dMAEs, which provides an opportunity to estimate the consequences of short MAEs for the storage phenomenon. Whether or not there is a meaningful difference between the results for the two speeds (of 11.28 and 19.74 deg/s) cannot be deduced from these data, but it is obvious that there is a difference in MAE-duration at these speeds between the subjects. We have remarked on this subject-dependence before and have illustrated the differences in speed-tuning characteristics between observers (e.g. Verstraten et al., 1998, Fig. 2, van de Grind et al., 2001, Fig. 2). This means once again that the practice of pooling data across large numbers of subjects can give misleading results, at least for the study of MAEs or their storage. Duration-data are inherently noisy and can often be replaced by more robust measures such as nulling-thresholds (see van de Grind et al., 2003), but given the definition of storage, there is no other means of directly measuring storage-strength than by using MAE-duration data. In the fourth panel in Fig. 8(D) we plotted the average duration data for each of the three subjects on the same scale, so that absolute dMAE-duration differences between subjects become manifest.

To test the model we took parameter values for the dMAE from van de Grind et al. (2003), who found that w is probably about 0.5, and τ about 3 s for the dMAE. With maximal adaptation $x_a = 10$ for $t_a = 30$ s, and a test signal strength x_t of around 1 (10% of full range), this leaves us with θ to explore whether or not we can fit the data. This was sufficient to fit the data of WG and

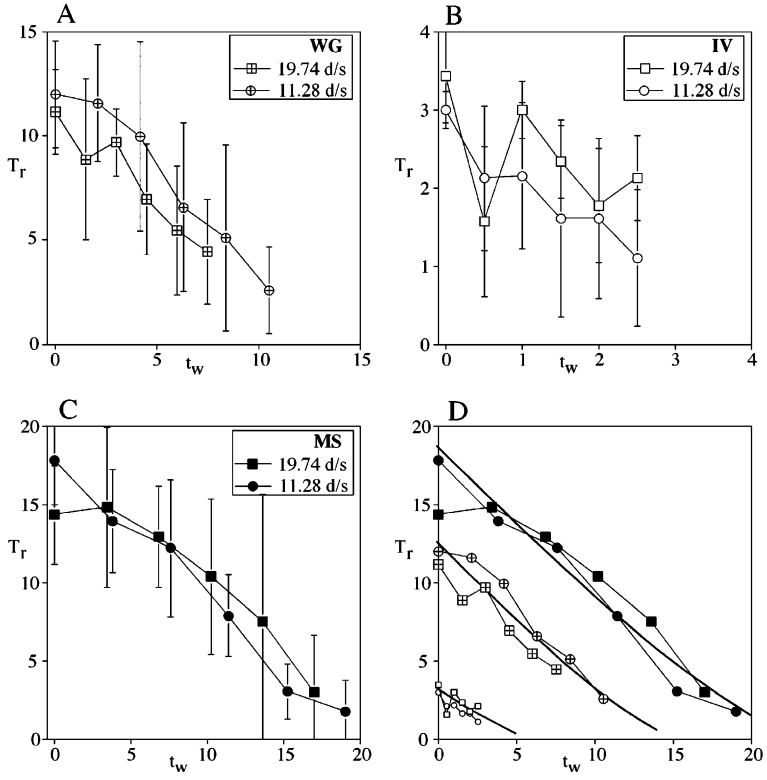

Fig. 8. Spigel functions for the dMAE at two adaptation speeds (19.74 and 11.28 deg/s), measured in our psychophysical experiment with moving RPAs, tested with 45 Hz dynamic spatial noise. The first three panels give the data for three observers (WG, IV, MS), each on their own ordinate scale, the fourth panel brings the data together on the same scale. Standard deviations are shown for each of the observers in their own panel and left out in the fourth panel. The fourth panel also shows model fits, calculated as described in the text.

IV, which will be discussed first. We did not attempt to find an optimal fit, since the noisiness of the data (Fig. 8A–C) makes this a futile exercise. Storage factor σ was first estimated from fitting a linear regression line through the data of subject WG, then we calculated the value of θ that would give us the same storage factor σ as found from the regression line. For WG this was $\theta = 0.032$. After that the corresponding Spigel-function was calculated and plotted as a thick curve in Fig. 8D. It is clear that the model describes the empirical findings very well. Next we tried to fit the data for IV by only changing criterion value θ. The value $\theta = 0.42$ gave a good fit (by eye), as illustrated in Fig. 8D. This means that the model suggests that IV has a 13 times higher criterion θ for seeing a dMAE, that is, if she has the same time constant of the gain-controls. Note that increasing only θ makes the Spigel curves less steep, since it increases storage (see Fig. 7). This is equivalent to moving vertically upwards in the diagrams of Figs. 4 and 7, that is to lowering the ratio T/τ. Observer IV, with the shortest dMAE-durations, indeed has the highest storage factor of the three subjects. If a 13 times higher criterion value seems too extreme, one can alternatively change τ- and w-values of the model description for this subject in such a way that a lower θ-value is obtained for the same storage factor. This is only possible because no independent measurements of parameters such as τ and w were available for her. This is one important general message of the present exercise in computational visual science: Without a model one is easily misled when interpreting psychophysical findings (which can lead to unnecessary complexities, such as a presumed 'storage' mechanisms). Similarly, one might presume that certain psychophysical data are self-sufficient (like storage measurements, averaged across subjects), whereas independent tests (e.g. to estimate τ) are in fact necessary per subject to really pin down the mechanisms underlying the phenomena.

Can we follow the same procedure to fit the data of MS, that is, just change θ? The answer is no. To get a longer MAE-duration one has to decrease θ, but that also steepens the Spigel function, and the data for MS show that this would not be appropriate. His curves indicate a similar storage as for WG. One way to solve this is to increase τ, the time constant of the gain-controls. This has no influence on storage factor σ (see above) but it gives a longer MAE-duration. By increasing τ from 3 to 5 s for MS we obtained a good fit of his results with $\theta = 0.036$, about the same threshold as for WG.

Now that we have adequate model descriptions of the data sets of the three subjects we can more easily answer

the question whether the dMAE shows storage and if so how much. The three parameter sets of the fitted Spigel functions correspond to storage factor values of 0.12, 0.11, and 0.38 for the three subjects MS, WG, and IV, respectively. This was again calculated with a Mathematica Notebook using formulae (5a)–(5e). The conclusions drawn from these results are:

1. Like an sMAE, the dMAE shows storage (σ-values from 0.1–0.4), but much less than the sMAE (which gives σ-values around 0.3–0.8);
2. The same basic MAE-model, a simple gain-control system, can explain both storage phenomena for static and dynamic MAEs;
3. The psychophysical results show major differences between subjects, a finding that speaks against pooling data across subjects. The model can translate these behavioral differences in differences of underlying parameter values, making it easier to study electrophysiological correlates.

6. Discussion

It seems only natural to assume that a MAE is caused by slowly but steadily decaying information on the preceding adaptation stimulus. This is indeed true for our formal model as well as for all informal models of the MAE presented in the literature (for a review, see Mather & Harris, 1998). With this in mind, the psychophysical finding called 'storage' then seems to involve a delay of recovery while the eyes are closed. This reasoning has seemed so obvious to most authors on the subject (including us in previous publications) that it started a search for special 'storage' mechanisms and led to the premature name for the phenomenon. The idea proposed in the present paper, that it is the test stimulus that speeds up gain equalization, rather than the absence of a stimulus that delays recovery, has been around as well. For example, Keck and Pentz (1977) have shown awareness of this possibility. They found that MAE decay depends strongly on the manipulation of test conditions and concluded from this (op.cit., p.723) that decay appears to be a combined effect of spontaneous recovery and of excitation by the test pattern.

Keck and Pentz (1977) thus formulated the principle on which the present, more formal, explanation is based. They realised that only a test stimulus of zero contrast would reveal the underlying time constant of recovery. By measuring recovery for different test contrasts and extrapolating the results to zero contrast they could estimate the rate of recovery in the absence of a test stimulus. The estimated time constants were around 20 s, which is close to the values we used above to describe Spigel's results. However, Keck and Pentz did not develop a quantitative model to explain and describe storage. Moreover, they relied heavily on relative speed estimation procedures, and it is not likely that there is a simple relation between perceived speed and MAE-duration (Hammett, Thompson, & Bedingham, 2000). In any case, the results of Keck and Pentz (1977), Thompson and Wright (1994), Verstraten et al. (1994b), and others, make it abundantly clear that 'storage' depends strongly on stimulus manipulations during the test phase. Our assumption that an effective test stimulus (one that makes a MAE visible) provides a non-selective stimulation of all direction-sensitive motion channels is at least compatible with these findings. The assumption is further supported by the fact that no MAE is normally seen with the eyes closed or if an inadequate stimulus (e.g. dynamic noise for a sMAE or a static pattern for a dMAE) is presented during the waiting-interval of a 'storage' experiment (Verstraten et al., 1994b).

If the test stimulus adapts motion sensors for all directions, as presumed in our model, the gains of all channels will converge on $1/(1 + wx_t)$ during prolonged testing or adaptation to the test stimulus. Very few students of MAEs have had the idea to measure the increase in motion-thresholds for adaptation to a static pattern, and this is exactly the experiment we need to test our postulate. Fortunately, Moulden and Mather (1978) and Pantle (1970) did the experiment. Pantle used static bar-gratings as adaptation stimulus, and the same gratings moving at speeds from 0 to 22 deg/s as threshold probes. Adaptation phases of 15 s were alternated with test phases of 1.5 s. He found that adaptation to the static grating increased the threshold for static or moving gratings compared to adaptation to a control stimulus of a homogeneous grey field. For low speeds the threshold increase was on the order of a factor 2, which means for our model that $1 + wx_t = 2$, so $wx_t = 1$. This is the order of magnitude we used in the above model studies (both w and x_t about 1). Moulden and Mather (1978) used sinewave gratings of 0.32 cpd moving at 7 deg/s to measure threshold increases after adaptation to a homogeneous field, a grating moving in the same, or in the opposite direction, or a static grating. We are here interested in the threshold increase due to adaptation to a static grating relative to that after adaptation to a uniform grey field. From their Table 1 on p. 516 we conclude that the log ratio threshold before and after adaptation to a static grating was 0.58 and after adaptation to a homogeneous field 0. Adaptation to a static grating thus increased the threshold by a factor of 3.8 ($= 10^{0.58}$). For our model this means $wx_t = 2.8$. In conclusion, our assumption that the static test stimuli in MAE-storage experiments adapt the responsible motion sensors is supported by these findings. It would of course be necessary in a comprehensive test of our model to measure such static adaptation phenomena for the same type of stimuli as used for 'storage' measurements and for determinations of τ. All

experiments would have to be done on the same subjects, preferably with sufficiently different MAE-durations. That would be a major undertaking that is clearly beyond the scope of the present paper.

Another effect, first described by Keck, Palella, and Pantle (1976), also finds its simplest explanation in our assumption of unselective stimulation and adaptation by the test stimulus. They found that a lower test contrast (of 1.7%) gives a longer-lasting sMAE than a higher test contrast (of 10.5%). This would be expected if a test stimulus shortens the MAE-duration more when it is stronger, as in our above model. The present model therefore neither requires a special 'storage' mechanism nor a separate explanation for the inverse test contrast effect on MAE-duration. They both follow from the idea that the test stimulus promotes recovery by equalizing the gains of all direction channels, leading to a faster equalization for a stronger test stimulus, despite the fact that the time constants of individual gain-controls are always the same. Barlow and Hill (1963) assumed that the MAE was a consequence of a temporary imbalance of the maintained discharges of opponently tuned motion sensors. If this were true one would also expect an MAE in the dark, which is not the case. Nevertheless, maintained or spontaneous activity of motion sensors might very well contribute, provided the contribution is perceptually subthreshold in the dark. In that case a fraction of our test stimulus strength x_t could be thought of as permanently present maintained neural activity, but too weak to generate a MAE without an additional test stimulus. Such a refinement has no principled consequences for the present explanation of storage-effects.

We have not attempted in this paper to include the front-end transformation from external visual stimuli to the internal model variables x_a and x_t. This is not necessary to explain the model's principles and to model 'storage' phenomenon. In a previous study (van de Grind et al., 2003) it was shown how the signal-to-noise ratio of random pixel arrays can be mapped onto the model's input variables. For sinewaves one could use a Naka–Rushton mapping formula, such as $x = Gc^n/(c_{50}^n + c^n)$, with n most probably about 2. Such a mapping assumption is necessary if one wants to relate stimulus contrast c (or other strength measures) to MAE-duration or nulling values. With such a mapping preceding our gain-controls we could indeed mimick the inverse contrast effect of Keck et al. (1976) in great detail (to be published elsewhere). Of course, the front-end luminance and contrast processing mechanisms in fact also contain gain-controls, with their own dynamic properties, making a static mapping (as described by a Naka–Rushton formula) a first-order non-dynamic approximation rather than a final description. In due course our model can be extended to also include front-end dynamic gain controls of luminance (e.g. van de Grind et al., 1996) and contrast signals.

In conclusion, we developed a model of the psychophysical MAE-'storage' phenomenon that does not require any special 'storage' mechanism apart from a steady recovery of automatic gain-controls after adaptation. In that sense one gets 'storage' for free. Only one recovery process is involved that does not change its time constant at all and that is never slowed down by anything. The *equalization* of gains of all direction tuned sensors is simply faster if the test stimulus is stronger and it is completed earlier if testing starts earlier. This is due to a non-selective stimulation of motion sensors by the test.

Acknowledgements

We thank Martin Lankheet, Ans Koenderink-van Doorn, Richard van Wezel, and Lothar Spillmann for critical reading and helpful discussions. F.V. is supported by a Pioneer grant of the Netherlands Organisation for Scientific Research (NWO). M.v.d.S. is supported by a grant of the Innovational Research Incentives Scheme (VENI) of the Netherlands Organisation for Scientific Research (NWO). W.v.d.G. is supported by the Deutsche Forschungsgemeinschaft (Mercator Guest Professorship at the Albert-Ludwigs University in Freiburg i.Br., Germany).

Appendix A

We start from the following four formulae, which were explained in the text (formulae (2)–(4)):

$$u^* = wx_a\{1 - \exp(-t_a/\tau)\}\exp(-t_w/\tau) \tag{A.1}$$

$$g_1 = 1/(1 + u_1) \quad \text{with}$$
$$u_1 = wx_t(1 - \exp[-t/\tau]) + u^* \exp[-t/\tau] \tag{A.2}$$

$$g_2 = 1/(1 + u_2) \quad \text{with } u_2 = wx_t(1 - \exp[-t/\tau]) \tag{A.3}$$

$$g_2 - g_1 = \theta/x_t \quad (\text{at } t = T_r) \tag{A.4}$$

(A.2) and (A.3) in (A.4) leads to

$$u_1 - u_2 = (1 + u_1)(1 + u_2)\theta/x_t \quad (\text{at } t = T_r) \tag{A.5}$$

Replacing t in (A.3) and (A.4) by T_r we get from this:

$$u^* \cdot E^{-1} \cdot x_t/\theta = \{1 + wx_t(1 - E^{-1}) + u^*E^{-1}\} \times \{1 + wx_t(1 - E^{-1})\} \tag{A.6}$$

where

$$E = \exp[T_r/\tau] \tag{A.7}$$

While E can neither be 0 (minimum value is 1) nor infinite, we can multiply both sides of Eq. (A.6) with E^2, leading to

$$Eu^*x_t/\theta = \{E + wx_t(E - 1) + u^*\}\{E + wx_t(E - 1)\}$$

which can be worked out to give:

$$E^2(1+wx_t)^2 - E\{(1+wx_t)(2wx_t-u^*)+u^*x_t/\theta\} + wx_t(wx_t-u^*)=0 \quad (A.8)$$

This formula is of the form $AE^2 - BE + C = 0$, with solution (in which $D = B^2 - 4AC$):

$$E = \{B \pm \sqrt{(D)}\}/2A$$

or with (A.7):

$$T_r/T = \mathrm{Ln}[\{B \pm \sqrt{(D)}\}/2A] \quad (A.9)$$

The terms A, B, C, and D are defined in the text in formulae (5b)–(5d). Only one of the two roots included in (A.9) consistently produces positive residual MAE-durations, namely

$$T_r/T = \mathrm{Ln}[\{B + \sqrt{D}\}/2A] \quad (A.10)$$

which is formula (5a) in the text.

To calculate curves of constant T/τ-values, as plotted in Figs. 4 and 7, one can use (A.8). For $T/\tau = \text{constant}$ we have $E = \text{constant} = k$, so we can replace E by k in (A.8) and solve for θ, which gives:

$$\theta = ku^*x_t/\{w^2x_t^2(k-1)^2 + wx_t(u^*+2k)(k-1) + k^2 + ku^*\} \quad (A.11)$$

With this formula we can plot θ as a function of w for any chosen constant value of T/τ, as in Figs. 4 and 7. For every pair of θ, w values we can then calculate the normalised residual MAE-duration for $t_w = T$, which we called T_{rT}/τ in the text. The ratio T_{rT}/τ to T/τ then gives us the storage factor σ for the chosen pair of θ, w values. All this is extremely cumbersome to do by hand, but very easy with programs like Mathematica, as used for the calculations in this paper.

References

Ashida, H., & Osaka, N. (1995a). Difference of spatial frequency selectivity between static and flicker motion aftereffects. *Perception, 23*, 1313–1320.

Ashida, H., & Osaka, N. (1995b). Motion aftereffect with flickering test stimuli depends on adapting velocity. *Vision Research, 35*, 1825–1833.

Barlow, H. B., & Hill, R. M. (1963). Evidence for a physiological explanation for the waterfall phenomenon and figural aftereffects. *Nature, 200*, 1345–1347.

Blake, R., & Hiris, E. (1993). Another means for measuring the motion aftereffect. *Vision Research, 33*, 1589–1592.

Carandini, M., & Ferster, D. (1997). A tonic hyperpolarization underlying contrast adaptation in cat visual cortex. *Science, 276*, 949–952.

Carandini, M., Heeger, D. J., & Movshon, J. A. (1997). Linearity and normalization in simple cells of the macaque primary visual cortex. *Journal of Neuroscience, 17*(21), 8621–8644.

van Doorn, A. J., Koenderink, J. J., & van de Grind, W. A. (1984). Limits in spatio-temporal correlation and the perception of visual movement. In A. J. van Doorn, W. A. van de Grind, & J. J. Koenderink (Eds.), *Limits in Perception* (pp. 203–234). Utrecht: VNU Science Press (Chapter 8).

van Doorn, A. J., Koenderink, J. J., & van de Grind, W. A. (1985). Perception of movement and correlation in stroboscopically presented noise patterns. *Perception, 14*, 209–224.

Exner, S. (1894). *Entwurf zu einer physiologischen Erklärung der psychischen Erscheinungen*. Wien: Deuticke.

Green, M., Chilcoat, M., & Stromeyer, C. F. (1983). Rapid motion aftereffect seen within uniform test fields. *Nature, 304*, 61–62.

Griffith, B. C., & Spitz, H. H. (1959). Some observations on the spiral aftereffect. *American Journal of Psychology, 72*, 139–140.

van de Grind, W. A., Grüsser, O.-J., & Lunkenheimer, H.-U. (1973). Temporal transfer properties of the afferent visual system: psychophysical neurophysiological and theoretical investigations. In R. Jung (Ed.), *Central Processing of Visual Information: vol. VII/3A. Handbook of Sensory Physiology* (pp. 431–573). Berlin: Springer Verlag (Chapter 7).

van de Grind, W. A., van Hof, P., van der Smagt, M. J., & Verstraten, F. A. J. (2001). Slow and fast visual motion channels have independent binocular rivalry stages. *Proceedings of the Royal Society, London B, 268*, 437–443.

van de Grind, W. A., Koenderink, J. J., & Bouman, M. A. (1970). Models of the processing of quantum signals by the human peripheral retina. *Kybernetik, 6*, 213–227.

van de Grind, W. A., Koenderink, J. J., van der Heyde, G. L., Landman, H. A. A., & Bouman, M. A. (1971). Adapting coincidence scalers and neural modelling studies of vision. *Kybernetik, 8*, 85–105.

van de Grind, W. A., Lankheet, M. J. M., & Tao, R. (2003). A gain-control model relating nulling results to the duration of dynamic motion aftereffects. *Vision Research, 43*, 117–133.

van de Grind, W. A., Lankheet, M. J. M, van Wezel, R. J. A., Rowe, M. H., & Hulleman, J. (1996). Gain control and hyperpolarisation level in cat horizontal cells as a function of light and dark adaptation. *Vision Research, 36*(24), 3969–3985.

von Grünau, M. W. (1986). A motion aftereffect for long-range stroboscopic apparent motion. *Perception & Psychophysics, 40*, 31–38.

Grunewald, A. (1996). A model of transparent motion and non-transparent motion aftereffects. In D. S. Touretzky, M. C. Mozer, & M. E. Hasselmo (Eds.), *Advances in Neural Information Processing Systems* (vol. 8, pp. 837–843). Cambridge, MA, USA: MIT Press.

Grunewald, A., & Lankheet, M. J. M. (1996). Orthogonal motion after-effect illusion predicted by a model of cortical motion processing. *Nature, 384*(6607), 358–360.

Hammett, S. W. T., Thompson, P. G., & Bedingham, S. (2000). The dynamics of velocity adaptation in human vision. *Current Biology, 10*, 1123–1126.

Hammond, P., Mouat, G. S. V., & Smith, A. T. (1988). Neural correlates of motion after-effects in cat striate cortical neurones: monocular adaptation. *Experimental Brain Research, 72*, 1–20.

Hiris, E., & Blake, R. (1992). Another perspective on the visual motion aftereffect. *Proceedings of the National Academy of Sciences USA, 89*, 9025–9028.

Keck, M. J., Palella, T. D., & Pantle, A. (1976). Motion aftereffect as a function of the contrast of sinusoidal gratings. *Vision Research, 16*, 187–191.

Keck, M. J., & Pentz, B. (1977). Recovery from adaptation to moving gratings. *Perception, 6*, 719–725.

Kohn, A., & Movshon, J. A. (2003). Neuronal adaptation to visual motion in area MT of the macaque. *Neuron, 39*, 681–691.

Ledgeway, T. (1994). Adaptation to second-order motion results in a motion aftereffect for directionally-ambiguous test stimuli. *Vision Research, 34*, 2879–2889.

Mather, G. (1980). The movement aftereffect and a distribution-shift model for coding the direction of visual movement. *Perception, 9*, 379–392.

Mather, G., & Harris, J. (1998). Theoretical models of the motion aftereffect. A modern perspective. In G. Mather, F. Verstraten, & S. Anstis (Eds.), *The motion aftereffect*. Cambridge, MA, USA: Bradford Book, The MIT Press (Chapter 7).

Mather, G., Verstraten, F., & Anstis, S. (1998). *The motion aftereffect. A modern perspective*. Cambridge, MA, USA: Bradford Book, The MIT Press.

Moulden, B., & Mather, G. (1978). In defence of a ratio model for movement detection at threshold. *Quarterly Journal of Experimental Psychology, 30*, 505–520.

McCarthy, J. E. (1993). Directional adaptation effects with constant modulated stimuli. *Vision Research, 33*, 1109–1112.

Niedeggen, M., & Wist, E. R. (1998). The physiologic substrate of motion aftereffects. In G. Mather, F. A. J. Verstraten, & S. Anstis (Eds.), *The motion aftereffect. A modern perspective*. Cambridge, MA, USA: Bradford Book, The MIT Press (Chapter 6).

Nishida, S., & Sato, T. (1995). Motion aftereffect with flickering test patterns reveals higher stages of motion processing. *Vision Research, 35*, 477–490.

Pantle, A. (1970). Adaptation to pattern spatial frequency: effects on visual movement sensitivity in humans. *Journal of the Optical Society of America, 60*(8), 1120–1124.

Sanchez-Vives, M. V., Nowak, L. G., & McCormick, D. A. (2000). Membrane mechanisms underlying contrast adaptation in cat area 17 in vivo. *Journal of Neuroscience, 20*, 4267–4285.

Sekuler, R. W., & Ganz, L. (1963). Aftereffect of seen motion with a stabilized retinal image. *Science, 139*, 419–420.

Sekuler, R., & Pantle, A. (1967). A model for after-effects of seen movement. *Vision Research, 7*, 427–439.

van der Smagt, M. J., Verstraten, F. A. J., & van de Grind, W. A. (1999). New transparent motion aftereffect. *Nature Neuroscience, 2*, 595–596.

Spigel, I. M. (1960). The effects of differential post-exposure illumination on the decay of a movement after-effect. *Journal of Psychology, 50*, 209–210.

Spigel, I. M. (1962a). Contour absence as a critical factor in the inhibition of the decay of a movement aftereffect. *Journal of Psychology, 54*, 221–228.

Spigel, I. M. (1962b). Relation of MAE duration to interpolated darkness intervals. *Life Sciences, 1*, 239–242.

Spigel, I. M. (1964). The use of decay inhibition in an examination of central mediation in movement aftereffects. *Journal of General Psychology, 70*, 241–247.

Sutherland, N. S. (1961). Figural aftereffects and apparent size. *Quarterly Journal of experimental Psychology, 13*, 222–228.

Thompson, P., & Wright, J. (1994). The role of intervening patterns in the storage of the movement aftereffect. *Perception, 23*, 1233–1240.

Verstraten, F. A. J., Fredericksen, R. E., & van de Grind, W. A. (1994a). Movement aftereffect of bi-vectorial transparent motion. *Vision Research, 34*, 349–358.

Verstraten, F. A. J., Fredericksen, R. E., Grüsser, O.-J., & van de Grind, W. A. (1994b). Recovery from motion adaptation is delayed by successively presented orthogonal motion. *Vision Research, 34*, 1149–1155.

Verstraten, F. A. J., van der Smagt, M. J., Fredericksen, R. E., & van de Grind, W. A. (1999). Integration after adaptation to transparent motion: static and dynamic test patterns result in different aftereffect directions. *Vision Research, 39*, 803–810.

Verstraten, F. A. J., van der Smagt, M. J., & van de Grind, W. A. (1998). Aftereffect of high-speed motion. *Perception, 27*, 1055–1066.

Wade, N. J. (1994). A selective history of the study of visual motion aftereffects. *Perception, 23*, 1111–1134.

Wohlgemuth, A. (1911). On the after-effect of seen movement. *British Journal of Psychology, 1*(Monogr Suppl), 1–117.